

Assessing Downscaling Techniques for Frequency Analysis, Total Precipitation and Rainy Days Estimation in CMIP6 Simulations over Hydrological Years

David A. Jimenez¹, Andrea Menapace², Ariele Zanfei³, Eber José de Andrade^{1,4}, Bruno Brentan¹

¹Hydraulic and Water Resources Department, Federal University of Minas Gerais UFMG, 31270-901, MG, Brazil

²Faculty of Science and Technologies, Free University of Bozen-Bolzano, 39100 Bolzano, Italy

³AIAQUA S.r.l., Via Volta 13/A, Bolzano, Italy.

⁴The Geological Survey of Brazil, 30140-002, MG, Brazil

Correspondence to: David A. Jimenez O. (dajimenezoo30@gmail.com)

Abstract. General circulation models generate **climate** simulations on grids with resolutions ranging from 50 km to 600 km. The resulting coarse spatial resolution **of the model outcomes requires post-processing routines to ensure reliable climate information for practical studies**, prompting the widespread application of downscaling techniques. However, assessing the effectiveness of multiple downscaling techniques is essential, as their accuracy varies depending **on the objectives of the analysis and the characteristics of the case study**. In this context, **this study aims to evaluate the performance of downscaling the daily precipitation series in the Metropolitan Region of Belo Horizonte, Brazil, with the final scope of performing frequency analyses, and estimating total precipitation and the number of rainy days per hydrological year at both annual and multiannual levels**. To develop this study, **78 climate models** with a horizontal resolution of 100 km, which participated in the SSP1-2.6 and/or SSP5-8.5 scenarios of CMIP6, are employed. The results highlight that adjusting the simulations from the general **circulation** models by Delta Method, Quantile Mapping, and Regression Trees produces **accurate results for estimating the total precipitation and number of rainy days**. Finally, it is noted that employing downscaled precipitation series through Quantile Mapping and Regression Trees yields **promising results also in terms of the frequency analyses**.

1 Introduction

As emphasised by the Intergovernmental Panel on Climate Change (IPCC), Global Climate Models (GCMs) represent the most advanced climate simulation tools and play a fundamental role in evaluating future climate scenarios (IPCC, 2014). GCMs have the capability to generate coherent climate estimations both physically and geographically. The GCMs are used to examine the effect of increasing greenhouse gas emissions on climatic variables (Ostad-Ali-Askari et al., 2020). However, due to their low spatial resolution (50-600 km), they are unable to adequately reproduce the climatic variables of small areas such as basins and sub-basins (Ozbuldu & Irvem, 2021), whereby the application of downscaling techniques has become a standard procedure (Worku et al., 2021; Olsson et al., 2016).

31 Downscaling aims to refine low-resolution global climate projections to local or regional scales by identifying relationships
32 between observed climate data and simulations from GCMs (Jimenez, 2022; Zhang & Li, 2020). Downscaling enhances the
33 representativeness of projected climate conditions, making them more accurate of local climate conditions. Ensuring adequate
34 downscaling is essential since adjusted series are employed to assess the impacts of climate change on regional scales
35 (Teutschbein et al., 2011). If an inadequate methodology of downscaling is selected for future climate projections,
36 misinterpretation and inaccurate estimation of the effects of climate change, with detrimental consequences for long-term
37 planning in the management of climate change impacts could be done (Rastogi et al., 2022). For instance, underestimating
38 regional-scale responses to climate change can result in a lack of preparedness from a planning and mitigation perspective.
39 Conversely, overestimating these responses can lead to an excessive budget allocation for addressing the consequences.

40 Given the variety of downscaling techniques available in the literature (Delta Method, Quantile Mapping, Machine Learning
41 Techniques, etc.), Rastogi et al. (2022), Yang et al. (2019), and Onyutha et al. (2016) report that the efficiency of downscaling
42 techniques varies depending on several reasons, such as the research objectives, the data and the case study, making it necessary
43 to evaluate multiple techniques in each specific study. The analysis and characterization of changes in precipitation patterns is
44 one of the most relevant thematic areas in research addressing the impacts of climate change. Mahla et al. (2019), Salehnia et
45 al. (2019), Yang et al. (2019), Sachindra et al. (2018) and Hashmi et al. (2011), evaluated the performance of downscaled
46 techniques to reduce precipitation.

47 Mahla et al. (2019) indicated that downscaling monthly precipitation based on multiple linear regressions showed promising
48 results for the study area. On the other hand, Salehnia et al. (2019) identified that Dynamic Downscaling (DDS) provides better
49 results than Statistical Downscaling (SDS) in total annual and seasonal precipitation downscaling, pointing out that SDS is
50 computationally simpler than DDS. Conversely, Yang et al., (2019), found that methods based on quantile mapping
51 demonstrate better performance in the downscaling of seasonal scale and extreme precipitation Compared to the function
52 transform method (CDF-t). Sachindra et al. (2018) recommended using a Regional Vector Machine (RVM) over Genetic
53 Programming (GP), Artificial Neural Networks (ANNs) and Support Vector Machine (SVM) for monthly precipitation
54 downscaling. Finally, Hashmi et al. (2011) identified that the GP provides better results for daily precipitation downscaling
55 than ANNs.

56 Most of the studies have focused on assessing the efficiency of downscaling techniques for monthly, annual, and seasonal
57 precipitation by the civil year (Kreienkamp et al., 2019; Ozbuldu & Irvem, 2021). However, only a few studies have been
58 conducted for the hydrological year. Instead, no studies were identified evaluating the effectiveness of these techniques for
59 conducting frequency analysis.

60 Tabari et al. (2021), Liu et al. (2020), Norris et al. (2020) and Hassanzadeh et. al. (2014) indicated that climate change could
61 transform or modify temperature and relative humidity patterns, leading to the intensification of extreme weather events (Roca

62 et al., 2019). Thus, authors such as Fadhel et al., (2017), Shahabul and Elshorbagy (2015) and Waters et al., (2003) emphasize
63 that in the current context of climate change, it is necessary to identify potential changes in Intensity-Duration-Frequency
64 (IDF) relationships.

65 Therefore, it is essential to assess the representativeness of downscaling techniques for conducting frequency analyses, because
66 the number of studies evaluating the alterations in IDF relationships in the climate change context from simulations of GCMs
67 has been increasing (e.g., Ghasemi Tousi et al. (2021), Hassanzadeh et al. (2014) and Hashmi et al. (2011)). The assessment
68 of changes in IDF relationships in climate change scenarios plays a fundamental role in decision-making related to the planning
69 of hydraulic infrastructure, drainage systems, flood prevention, and water resource management. Identifying these changes
70 enables authorities, engineers, and planners to incorporate the new climate realities into the development of infrastructure
71 projects.

72 To ensure accurate downscaling and enable a correct estimation and interpretation of the impacts of climate change on IDF
73 relationships, the proposed work aims to investigate the performance of some of the most recognized downscaling techniques
74 in the literature, such as the Delta Method (DM), Quantile Mapping (QM), and Regression Trees (RT), in terms of frequency
75 analysis. Additionally, the techniques were also evaluated for their ability to reproduce total precipitation and the number of
76 rainy days per hydrological year and at a multiyear level.

77 In this way, the present study contributes to the identification and selection of downscaling techniques that can be applied in
78 research **that assessing changes** in IDF relationships from CMIP6 projections, as well as in studies evaluating changes in the
79 number of rainy days and total precipitation **at the multiyear level** in the context of climate change. In order to facilitate the
80 paper's understanding, the second section presents the study area, the data used, the downscaling techniques considered, and
81 the efficiency metrics used to evaluate the downscaling techniques. The third section presents the results and discussion, while
82 the fourth section draws the conclusions and final considerations.

83 **2. Data and Methodology**

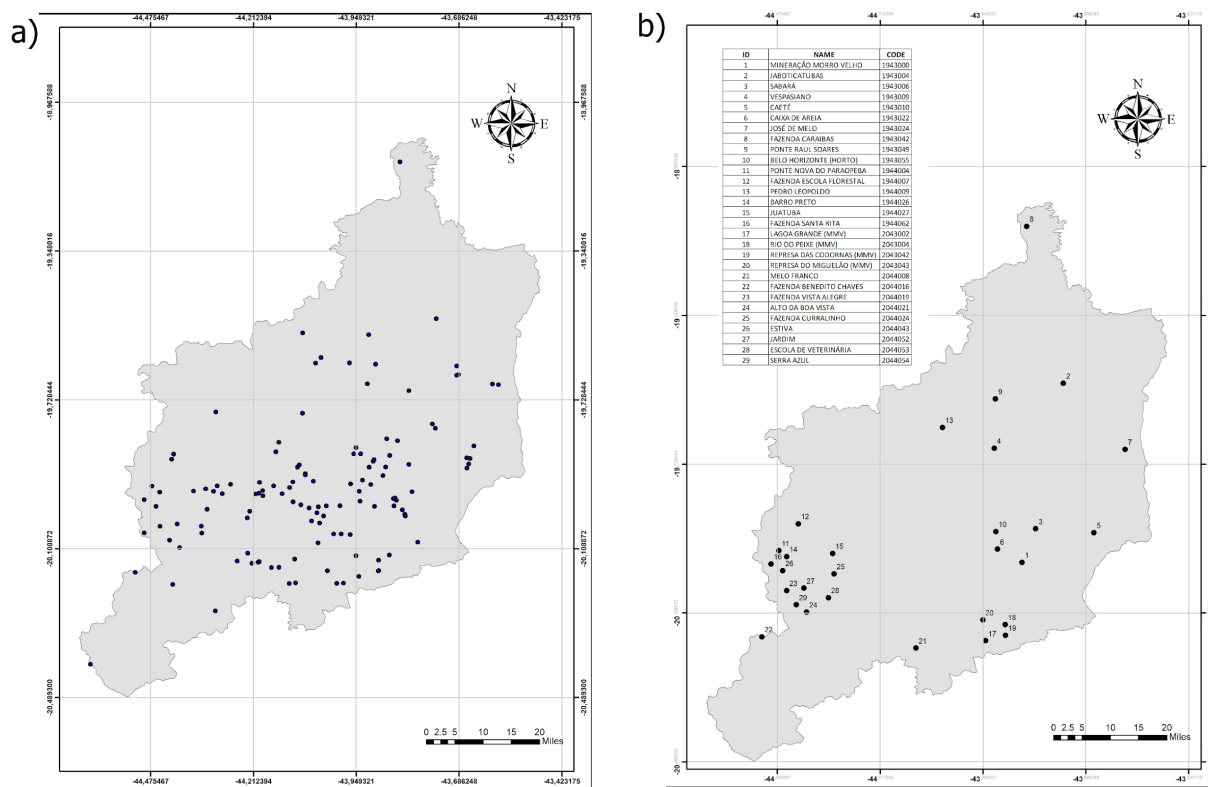
84 **2.1 Study Area and historical rainfall records**

85 The study was conducted in the Metropolitan Region of Belo Horizonte (MRBH), which is located between latitudes 18.0°
86 and 20.5° south and longitudes 43.15° and 44.75° east, in the central region of the state of Minas Gerais, Brazil. The MRBH
87 covers an area of 9468 km² with a hydrological year starting in October, with precipitation **occurring** from October to March.
88 Monthly precipitation can exceed 300 mm/month. The MRBH monitoring network comprises more than 120 pluviometric
89 stations distributed throughout the region (**see** Figure 1a).

90 The MRBH is selected because, as Nunes (2018) indicated, a significant portion of MRBH is directly or indirectly experiencing
 91 the consequences of extreme rainfall events. Between 1928 and 2000, 200 floods were recorded in Belo Horizonte, with 69.5%
 92 of these events occurring in the last two decades analysed. Furthermore, over 37 flood events were reported between 2000 and
 93 2020.

94 The rainfall records for the MRBH are obtained from the Hydrological Information System (Hidroweb) of the Brazilian
 95 National Water Agency, available at <https://www.snirh.gov.br/hidroweb/serieshistoricas>. Upon downloading the rainfall data,
 96 we ensured its consistency by constructing double mass curves using total precipitation data for each hydrological year.
 97 **Rainfall stations with over 30 years of consistent records and with missing data below 10% were selected.** It is important to
 98 note that we did **not fill in any missing data**, as this could introduce uncertainties in the results.

99 Double mass curves are processed to perform consistency analysis on the collected data. Stations with distances less than 44
 100 km and a correlation equal to or greater than 0.7 from each reference station were selected to perform this calculation. **It was**
 101 **evident that only 29 stations have more than 30 years of consistent records and missing data below 10%.** Thus, the study was
 102 developed from the rainfall information of the 29 stations shown in Figure 1b.



103
 104 **Figure 1 Pluviometric stations of MRBH: a) monitoring network of pluviometric stations and b) selected pluviometric**
 105 **stations used in the present study.**

106 2.2 Simulation of rainfall conditions

107 The daily precipitation data simulated for the historical period (1850-2014) by GCMs with the resolution of 100 km,
 108 participating in emission scenarios SSP1-2.6 and/or SSP5-8.5 of CMIP6, were obtained from [https://esgf-](https://esgf-node.llnl.gov/search/cmip6/)
 109 [node.llnl.gov/search/cmip6/](https://esgf-node.llnl.gov/search/cmip6/). It is important to emphasize that all available simulations with a resolution of 100 km have been
 110 included to consider all the ensembles available for each climate model. This choice was made with the intention of utilizing
 111 all available model outputs and thus providing a more robust analysis.

112 The SSP5-8.5 and SSP1-2.6 scenarios are selected as the CMIP6 scenarios that project the highest and lowest temperature
 113 increases respectively. In the case of SSP5-8.5 scenario, it is assumed that the economic and social development of humankind
 114 until the end of the 21st century will be governed by: i) high exploitation of resources, ii) intensive use of fossil fuels, iii) high
 115 global energy demand. All these factors lead to high greenhouse gas concentrations, resulting in a radiative forcing of 8.5 W
 116 m⁻² by the end of the 21st century (Riahi et al., 2016). On the other hand, SSP1-2.6 scenario considers that: i) the world is
 117 turning towards sustainability, ii) there is a commitment by nations to reduce social inequalities, iii) consumption is oriented
 118 towards low material growth and low resource and energy consumption. All these factors were combined with a radiative
 119 forcing of 2.6 W m⁻² (Riahi et al., 2016). The simulations contemplated are presented in Table 1.

120

121 Table 1 Overview of the CMIP6 GCM ensemble used in this study (r –realisation or ensemble member; i –initialisation
 122 method; p–physics; f–forcing).

123

ID	Model	Ensamble	SSP1-2.6 future	SSP5-8.5 future
1	CESM2	r1i1flp1	X	✓
2	CESM2	r4iflp1	✓	X
3	CESM2-WACCM	r1ilflp1	X	✓
4	CESM2-WACCM	r2ilflp1	X	X
5	CESM2-WACCM	r3ilflp1	X	✓
6	CMCC-CM2-SR5	r1ilflp1	✓	✓
7	CMCC-ESM2	r1ilflp1	✓	✓
8	EC-Earth3-CC	r1ilflp1	X	✓
9	EC-Earth3	r10i1p1fl	✓	✓
10	EC-Earth3	r102i1p1fl	✓	✓
11	EC-Earth3	r103i1p1fl	✓	✓
12	EC-Earth3	r104i1p1fl	✓	✓
13	EC-Earth3	r105i1p1fl	✓	✓
14	EC-Earth3	r106i1p1fl	✓	✓
15	EC-Earth3	r107i1p1fl	✓	✓
16	EC-Earth3	r108i1p1fl	✓	✓

ID	Model	Ensamble	SSP1-2.6 future	SSP5-8.5 future
17	EC-Earth3	r109i1p1fl	✓	✓
18	EC-Earth3	r110i1p1fl	✓	✓
19	EC-Earth3	r111i1p1fl	✓	✓
20	EC-Earth3	r112i1p1fl	✓	✓
21	EC-Earth3	r113i1p1fl	✓	✓
22	EC-Earth3	r114i1p1fl	✓	✓
23	EC-Earth3	r115i1p1fl	✓	✓
24	EC-Earth3	r116i1p1fl	✓	✓
25	EC-Earth3	r117i1p1fl	✓	✓
26	EC-Earth3	r118i1p1fl	✓	✓
27	EC-Earth3	r119i1p1fl	✓	✓
28	EC-Earth3	r11i1flp1	✓	✓
29	EC-Earth3	r121i1p1fl	✓	✓
30	EC-Earth3	r122i1p1fl	✓	✓
31	EC-Earth3	r123i1p1fl	✓	✓
32	EC-Earth3	r124i1p1fl	✓	✓

ID	Model	Ensamble	SSP1-2.6 future	SSP5-8.5 future
33	EC-Earth3	r125i1p1fl	✓	✓
34	EC-Earth3	r126i1p1fl	✓	✓
35	EC-Earth3	r127i1p1fl	✓	✓
36	EC-Earth3	r128i1p1fl	✓	✓
37	EC-Earth3	r129i1p1fl	✓	✓
38	EC-Earth3	r130i1p1fl	✓	✓
39	EC-Earth3	r131i1p1fl	✓	✓
40	EC-Earth3	r132i1p1fl	✓	✓
41	EC-Earth3	r133i1p1fl	✓	✓
42	EC-Earth3	r134i1p1fl	✓	✓
43	EC-Earth3	r135i1p1fl	✓	✓
44	EC-Earth3	r136i1p1fl	✓	✓
45	EC-Earth3	r137i1p1fl	✓	✓
46	EC-Earth3	r138i1p1fl	✓	✓
47	EC-Earth3	r139i1p1fl	✓	✓
48	EC-Earth3	r13i1p1fl	✓	✓
49	EC-Earth3	r140i1p1fl	✓	✓
50	EC-Earth3	r141i1p1fl	✓	✓
51	EC-Earth3	r142i1p1fl	✓	✓
52	EC-Earth3	r143i1p1fl	✓	✓
53	EC-Earth3	r144i1p1fl	✓	✓
54	EC-Earth3	r145i1p1fl	✓	✓
55	EC-Earth3	r146i1p1fl	✓	✓

ID	Model	Ensamble	SSP1-2.6 future	SSP5-8.5 future
56	EC-Earth3	r147i1p1fl	✓	✓
57	EC-Earth3	r148i1p1fl	✓	✓
58	EC-Earth3	r149i1p1fl	✓	✓
59	EC-Earth3	r150i1p1fl	✓	✓
60	EC-Earth3	r15i1p1fl	✓	✓
61	EC-Earth3	r1i1flp1	✓	✓
62	EC-Earth3	r3i1flp1	X	✓
63	EC-Earth3	r4i1flp1	✓	✓
64	EC-Earth3	r6i1flp1	✓	✓
65	EC-Earth3-Veg	r1i1flp1	✓	✓
66	EC-Earth3-Veg	r2i1flp1	X	✓
67	EC-Earth3-Veg	r3i1flp1	✓	✓
68	EC-Earth3-Veg	r4i1flp1	✓	✓
69	EC-Earth3-Veg	r6i1flp1	✓	✓
70	GFDL-CM4	r1i1flp1	X	✓
71	GFDL-ESM4	r1i1flp1	✓	✓
72	INM-CM4-8	r1i1flp1	✓	✓
73	INM-CM5-0	r1i1flp1	✓	✓
74	MPI-ESM1-2-HR	r1i1flp1	✓	✓
75	MPI-ESM1-2-HR	r2i1flp1	✓	✓
76	MRI-ESM2-0	r1i1flp1	✓	✓
77	NorESM2-MM	r1i1flp1	✓	✓
78	TaiESM1-R1	r1i1flp1	✓	✓

124

125 2.3 Downscaling

126 The primary approaches to downscaling are SDS and DDS. In this study, two of the most popular SDS techniques were
127 evaluated: the Delta Method, Quantile Mapping, as well as the ML-Method Regression Trees. Due to their simplicity and low
128 computational effort, DM and QM have been widely used in many research studies. **In the case of DM, the investigations**
129 **developed by Salehnia et al., (2020), Salehnia et al., (2019) and Teutschbein & Seibert (2012) are noteworthy.** The study
130 developed by Salehnia et al., (2020) aims to investigate the impact of climate change on rainfed wheat yield in the Khorasan-
131 e Razavi province of northeast Iran. The study used climate projections from GCMs to assess the potential impact of climate
132 changes on rainfed wheat yield over the next decades (2019–2038). The DM was used to correct the simulations of temperature
133 and precipitation **on the daily and monthly scales.** On the other hand, Salehnia et al., (2019), compared the performance of DM
134 and DDS in terms of the amount and number of wet days, and total precipitation at annual and seasonal scales. The results
135 showed that DDS has better performance than DM. Similarly, it is highlighted that DM underestimates the annual mean

136 precipitation and the number of wet days, while DDS overestimates them. Finally, Teutschbein & Seibert (2012) compared
137 the performance of different downscaling techniques to correct precipitation and temperature. Their results highlighted that
138 the Delta Method is a stable and robust method, with the ability to produce future time series with dynamics similar to current
139 conditions. However, the method does not consider potential changes in future climatic dynamics.

140 With respect to QM, the studies conducted by Enayati et al. (2021), Heo et al. (2019), and Jakob Themeßl et al. (2011) are
141 noteworthy. In the study conducted by Enayati et al. (2021), the capability of bias correction in precipitation and temperature
142 simulations of GCMs using QM technique was evaluated. The results indicated that non-parametric methods of Quantile
143 Mapping exhibited the best performance. On the other hand, Heo *et al.* (2019), evaluated the use of different probability
144 distributions in QM, and the results showed that the selection of the probability distribution could lead to better or worse
145 results. Finally, Jakob Themeßl et al. (2011) indicated that the use of quantile mapping has better performance in the estimation
146 of high quantiles. In this way, the use of this technique could present an advantage in the case of extreme precipitation events.

147 In the case of RT, the studies conducted by Khalid and Sitanggang (2022) and Hutengs and Vohland (2016) stand out. Khalid
148 and Sitanggang (2022) compared various ML methods for downscaling precipitation, yielding that RT performed best. On the
149 other hand, the study conducted by Hutengs and Vohland (2016) adopted RT to enhance the spatial resolution of temperature
150 based on land surface temperature and reflectance with favourable results.

151 A Pixel-Station downscaling approach was developed. Observational data from each station were collected along with
152 simulated GCM data, extracted from the pixel containing that station. For all the selected pairs of time series, the temporal
153 consistency between daily precipitation observed and simulated was guaranteed by selecting the simulated data only for the
154 day in which the observation data are presented. Once the simulated series was obtained, the evaluated downscaling techniques
155 were applied for each selected point.

156 2.3.1 Delta Method

157 In this method, differences or 'deltas' between observed and GCM-simulated climatic conditions in the historical period are
158 calculated. Subsequently, assuming that these differences or deltas remain constant over time, they are applied to GCMs-
159 simulated future climate projections, thus refining climate projections at local or regional levels. The mathematical equation
160 employed by the Delta method is presented below:

$$161 P_{SD}^{Delta} = P_{Mod,daily} \left(\frac{P_{obs}}{P_{Mod}^{Monthly}} \right) \quad (2)$$

162 Where: P_{SD}^{Delta} represents the downscaled precipitation, $P_{Mod,daily}$ represents the simulated precipitation by the GCMs, \underline{P}_{obs}
163 represents the average monthly precipitation of the station and \underline{P}_{Mod} represents the average monthly precipitation simulated
164 by GCMs.

165 2.3.2 Quantile Mapping

166 QM is based on the principle of matching the quantiles of observed and GCMs-simulated distributions. The process begins
167 with estimating the quantiles of the observed series. Then, for the future period, the empirical probability associated with the
168 quantile simulated by the GCMs is estimated. This probability is used in the inverse probability function of observed quantiles,
169 thus obtaining the downscaled value. The following is a mathematical description of the method of precipitation:

$$P_{SD}^{QQ} = F_o^{-1}[F_M(P_M)] \quad (1)$$

170

171 where P_{SD}^{QQ} is the precipitation with *downscaling*, F_o^{-1} is the inverse empirical probability function of daily precipitation for
172 the historic period, F_M is the empirical probability function of simulated precipitation, and P_M is the simulated precipitation by
173 MCGs.

174 2.3.3 Regression Trees

175 Regression Trees are a Machine-Learning technique used to build predictive models. These models are created by recursively
176 dividing the sample space and adjusting predictive models for each subdivision (Loh, 2011). The main goal of this technique
177 is to partition the sample space into k units and create a predictive model for each subspace. This approach enables the
178 prediction of the variable of interest, Y, using a piecewise function of the type:

$$Y = \begin{cases} f_{E_0}(x), & x \in E_0 \\ f_{E_1}(x), & x \in E_1 \\ \dots \\ f_{E_k}(x), & x \in E_k \end{cases} \quad (3)$$

179

180 Where: Y is the predicted variable, $f_{E_i}(x)$ is the predictive model of the sample subspace E_i , and x is the predictor variable.

181 Downscaling using RT can incorporate more than one predictor variable to estimate the variable of interest, for example,
182 precipitation could be estimated using multiple variables simulated by General Circulation Models, such as temperature,
183 atmospheric pressure, and precipitation. However, it's important to note that the uncertainties in downscaling tend to increase
184 with the number of predictors. In this way, only daily precipitation is simulated as the predictor variable to minimize these
185 uncertainties.

186 The downscaling process was carried out using observed and simulated precipitation quantiles. This approach is used due to
187 the absence of a consistent temporal correlation between the observed and simulated rainfall magnitudes. Often, the simulated
188 precipitation by the GCMs did not match with the historical records, leading to instances where GCMs projected rainfall on
189 days when historical data indicated dry weather conditions. In the training stage, 85% of the records were used, while in the
190 validation stage, 15% were employed. The optimization of hyperparameters (Maximum number of splits, Split criterion) was
191 conducted using the automatic hyperparameter optimization function available in the 'fitree' function in Matlab.

192 **2.4 Frequency Analysis**

193 The frequency analysis is carried out using the maximum annual precipitation series, estimated from both historical records
194 and downscaling results. Initially, the stationarity and homogeneity of the maximum series are confirmed using the Spearman
195 (NERC, 1975) and Mann-Whitney (1947) statistical tests. These tests are applied at a 5% significance level, as specified by
196 Naghettini and Pinto (2007).

197 The frequency analysis is exclusively conducted on the series that exhibited homogeneity and stationarity. This analysis
198 considered various probability distributions, including Exponential, Gamma, Gumbel, GEV, Log-Normal, Pearson III, and
199 Log-Pearson III. The parameters for these distributions are estimated using L-moments method (Hosking, 1997). To evaluate
200 the adherence of the series to these probability distributions, the nonparametric Kolmogorov-Smirnov test is applied at a
201 significance level of 5%. For each station, the quantiles of precipitation associated with return periods of 2, 5, 10, 15, 30, 35,
202 45, 50, 60, 70, 80, 90, and 100 years were estimated based on the distribution that exhibited the best fit.

203 **2.5 Comparison between estimates made with historical series and downscaling.**

204 The efficiency of downscaling techniques was assessed in terms of total precipitation (TP) and the number of rainy days (RD)
205 at both the hydrological year and multiyear level. In the latter case, the total precipitation and rainy days are aggregated over
206 the available record period. **Similarly, the techniques are examined in terms of frequency analysis.**

207 The TP and RD by the hydrological year are evaluated using the Nash-Sutcliffe (NSE), Kling-Gupta (KGE), root-mean-square
208 error (RMSE), and the Pearson correlation coefficient (R). **In the case of the multiyear level, the evaluation was performed
209 using the percentage error.**

210 Nash-Sutcliffe (1979) and Gupta et al. (2009) indicated that NSE and KGE values of 1 represent an ideal match between
211 observed and simulated data. In the case of RMSE, a value of 0 signifies a perfect fit. Moreover, the R value, which falls
212 between 0 and 1, indicates a positive correlation. Values between -1 and 0 suggest a negative correlation, while those near 0
213 imply no correlation. Finally, a percentage error value of 0 indicates a perfect fit between observed and simulated data. The
214 equations used to calculate NSE, KGE, RMSE, R and percentage error are provided below:

$$NSE = 1 - \frac{\sum_{i=1}^n (X_i - X'_i)^2}{\sum_{i=1}^n (X_i - \bar{X}_i)^2} \quad (4)$$

$$KGE = 1 - \sqrt{(r - 1)^2 + \left(\frac{\sigma'_i}{\sigma_i} - 1\right)^2 + \left(\frac{\bar{X}'_i}{\bar{X}_i} - 1\right)^2} \quad (5)$$

$$RMSE = \sqrt{\frac{\sum_{i=1}^n (X_i - X'_i)^2}{n}} \quad (6)$$

$$R = \frac{n(\sum X_i X'_i) - (\sum X_i * \sum X'_i)}{\sqrt{[n(\sum X_i^2) - (\sum X_i)^2] * [n(\sum X_i'^2) - (\sum X'_i)^2]}} \quad (7)$$

$$\% Error = \frac{|X'_i - X_i|}{X_i} * 100 \quad (8)$$

215 Where X_i and X'_i are the observed and simulated values, while \bar{X}_i and \bar{X}'_i the mean of the observed and simulated values,
 216 respectively. n represents the number of simulated data, σ'_i the standard deviation of the simulated values, σ_i the standard
 217 deviation of the observed records, and R the correlation coefficient between the observed and simulated records.

218 3. Results and discussions

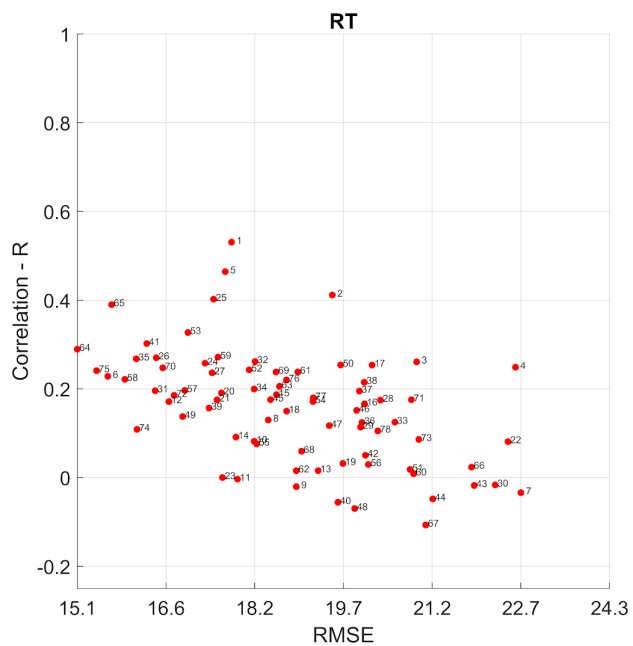
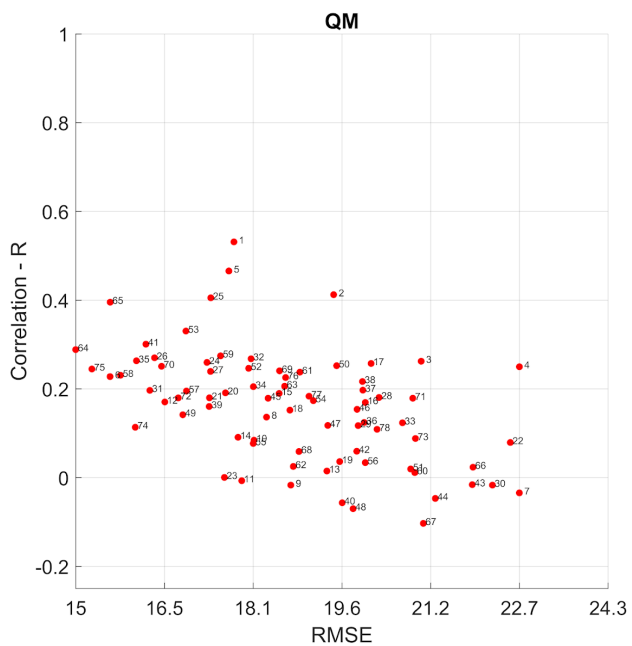
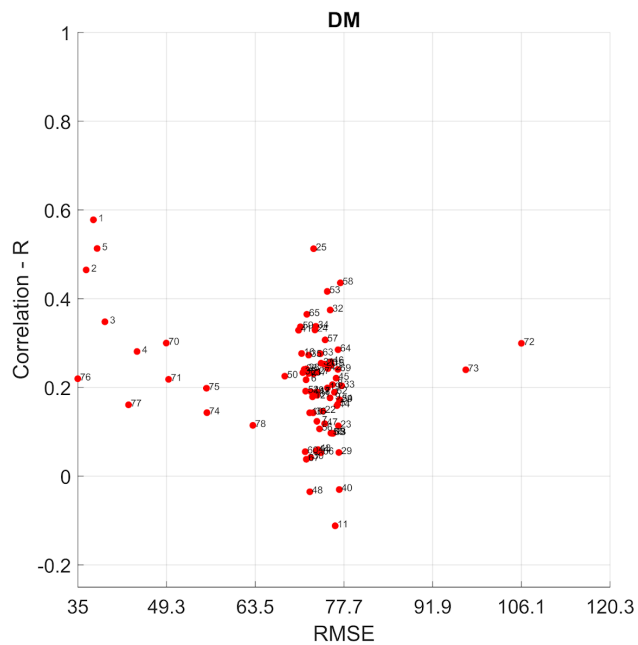
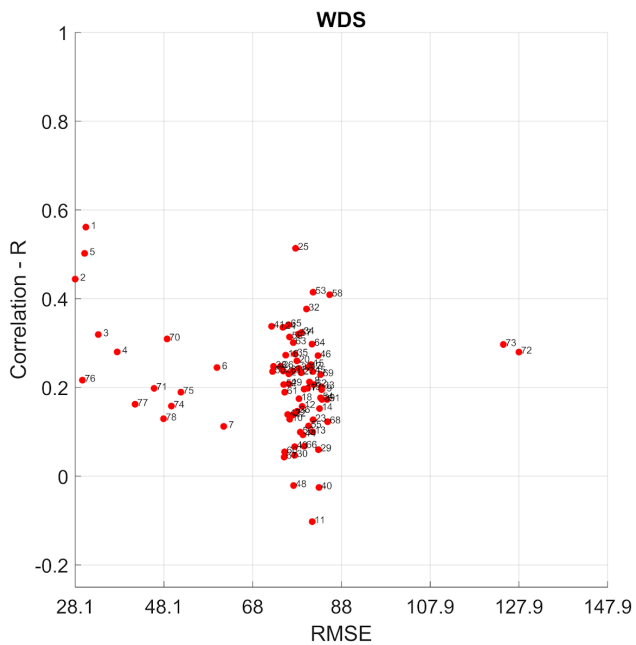
219 3.1 Total precipitation and number of rainy days per hydrological year

220 78 analyses were conducted both for total precipitation for the hydrological year and the number of rainy days, the median
 221 values of NSE, KGE, RMSE, and R were computed to facilitate the analysis and interpretation of the results, emphasizing that
 222 the median was chosen because it is less susceptible to extreme events.

223 Number of Rainy Days per hydrological year

224 Estimating the number of rainy days in the hydrological year, from downscaled series using DM, QM, and RT methods yields
 225 unsatisfactory results in all evaluated models. Thus, Figure 2 and Table 2 reveal discrepancies in the number of rainy days
 226 estimated per hydrological year from the downscaled series compared to observations. Without the application of any
 227 downscaling technique (WDS), this difference is approximately 78 days. However, when using DM, QM, and RT as
 228 downscaling techniques, the difference decreases to 73, 18, and 19 days, respectively. Thus, QM and RT stand out for providing
 229 the greatest reduction in the discrepancy between the number of rainy days per hydrological year estimated from the
 230 downscaled series compared to observations. Nonetheless, as mentioned and observed in Table 2 and Figure 2, the low NSE,
 231 KGE, and R scores show that the estimation of the number of rainy days at the annual scale does not work well.

232



233

234 Figure 2 Median performance metrics (RMSE and R) for the estimated number of rainy days from precipitation series
 235 simulated by GCMs, without the application of downscaling techniques (WDS), as well as adjusted series obtained using the
 236 DM, QM, and RT.

237 Table 2 Summary of performance metrics for estimating the number of rainy days from **without downscaling** and reduced
 238 series using DM, QM, and RT methods.

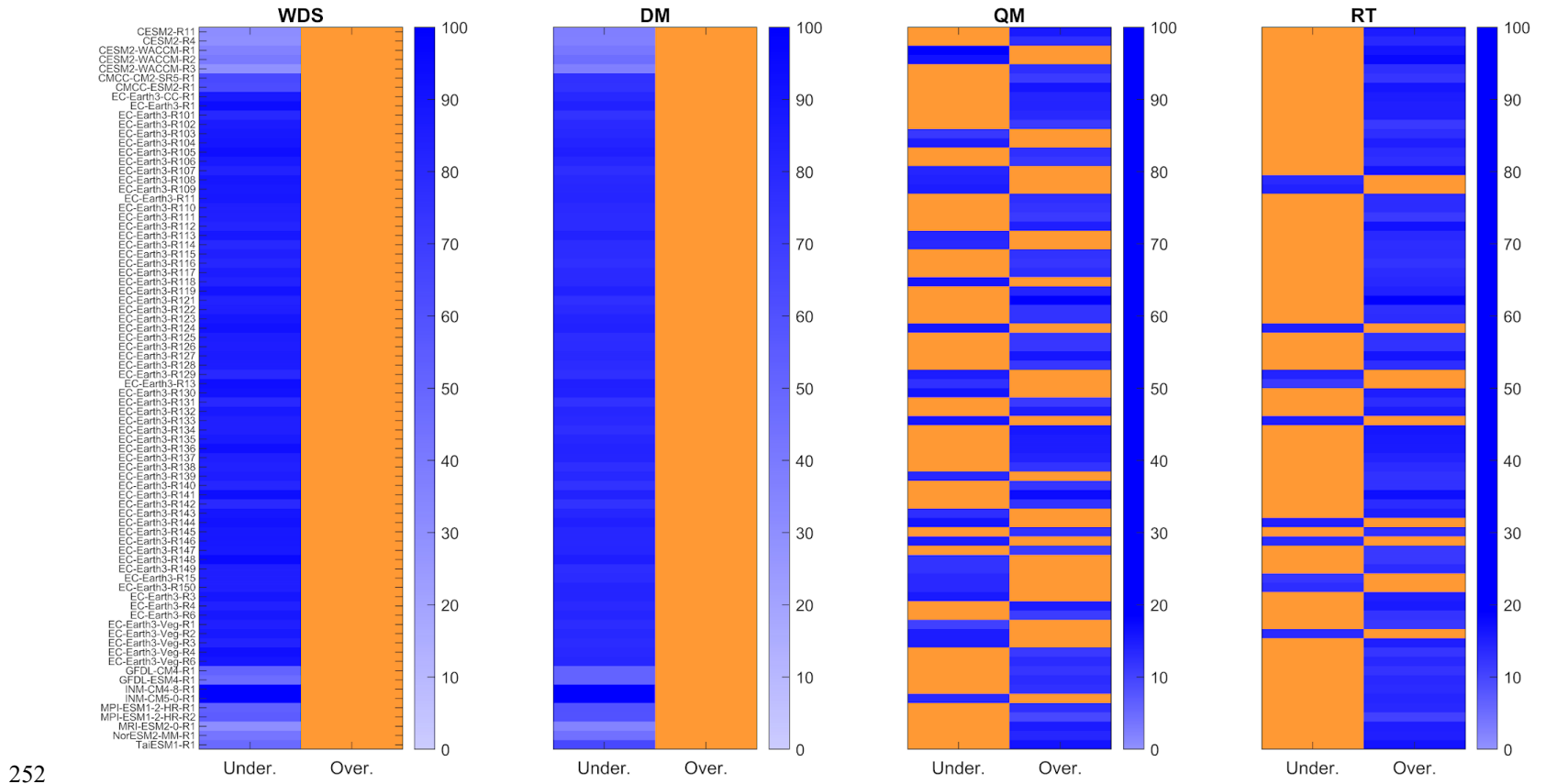
	WDS			DM			QM			RT		
	NSE	RMS E	KG E	NSE	RMS E	KG E	NSE	RMS E	KG E	NSE	RMS E	KG E
Maximum	-2.3	128	0.3	-4.5	106	0.2	-	23	0.44	-	23	0.44
Median	-44.2	78	-0.4	39.0	73	-0.4	-	18	0.05	-	19	0.05
Minimum	-	28	-0.8	-	35	-0.7	-	15	-0.21	-	15	-0.20

239

240 As shown in Figure 3, the low performance of NSE, KGE observed in the Table 2 in the estimation of number of rainy days
 241 per **hydrological** year, is associated with underestimations or overestimations.

242 As observed in Figure 3, an underestimation of the number of rainy days occurs when no downscaling techniques are applied.
 243 This underestimation trend persists when the DM is applied, consistent with the results found by Salehnia et al., (2019).
 244 However, when using QM and RT, this trend reverses, resulting in overestimation. **The persistence of underestimation when**
 245 **DM is applied may be related to the method of applying a constant correction factor per month.** On the other hand, the shift
 246 from underestimation to overestimation when using QM and RT can be attributed to the relationship between simulated and
 247 observed quantiles. Therefore, it is possible that there is a reclassification of dry days ($P \leq 1.0$ mm) as wet days ($P > 1.0$ mm)
 248 (i.e., a simulated quantile of 0.2 mm can be associated with observed precipitation > 1 mm).

249 The median percentage underestimation errors were 85.21%, 79.3%, 14.50%, and 13.70% for WDS, DM, QM, and RT,
 250 respectively. Meanwhile, the average overestimations were 12.54% and 13.78% for QM and RT, respectively.



252

253 Figure 3 Median percentage error of underestimation or overestimation of total number of rainy days per hydrological year. The percentage error
 254 of the prevailing condition of underestimation (Under.) or overestimation (Over.) is represented in blue, while the non-prevailing condition is
 255 depicted in orange. For example, if underestimation is prevalent, overestimation is represented in orange. WDS represents the condition without
 256 the application of downscaling techniques, DM corresponds to the condition when Delta Method is applied, QM represents the condition when
 257 Quantile Mapping is applied, and RT indicates the condition of applying Regression Trees as a downscaling technique.

258 **Total precipitation per hydrological year**

259 Estimating the total precipitation per hydrological year from the downscaled series obtained through the application of DM,
 260 QM, and RT does not guarantee good results. Thus, when no downscaling technique is applied, the difference between the
 261 total precipitation estimated from the downscaled series differs, on median 413.84 mm. In the case where DM is applied, this
 262 difference decreases to approximately 361.42 mm. However, when QM and RT are applied, the differences are higher than
 263 when no downscaling technique is applied, with median differences of 433.10 mm and 434.64 mm, respectively (see Figure
 264 4). That way, the difference between the total precipitation estimated from the downscaled series by QM and RT increases by
 265 approximately 4% compared to the estimations when no downscaling technique is applied and decreases by 12% when the
 266 DM is applied.

267 On the other hand, the low NSE, KGE, and R scores, as shown in Figure 4, indicate that the estimation of total precipitation at
 268 the annual scale from the downscaled series does not perform well.

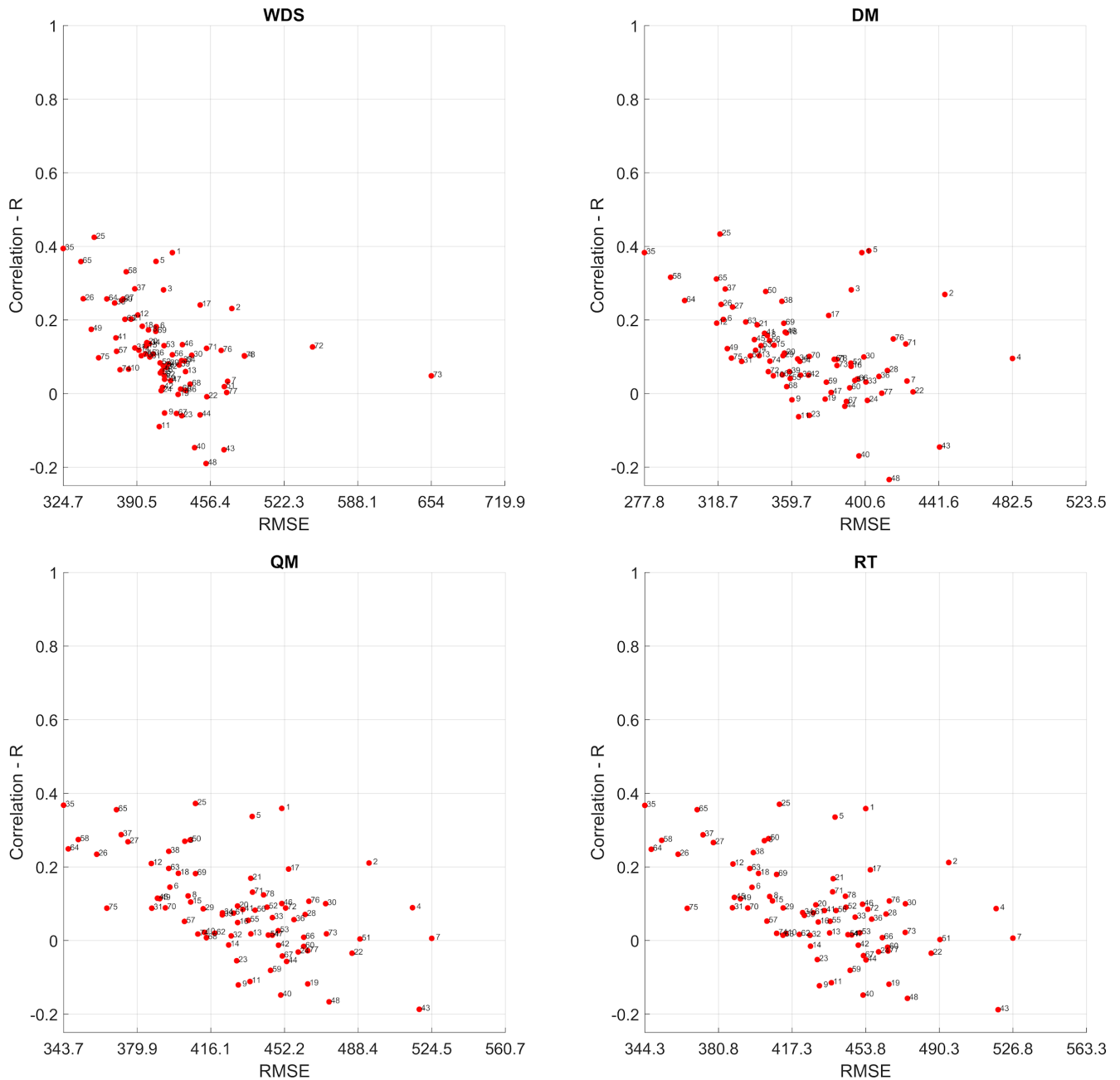
269 **Table 3 Summary of performance metrics for estimating the total precipitation by hydrological year without downscaling**
 270 **(WDS) and with DM, QM, and RT methods.**

	WDS			DM			QM			RT		
	NSE	RMSE	KGE	NSE	RMSE	KGE	NSE	RMSE	KGE	NSE	RMSE	KGE
Maximum	-0.53	654.02	0.36	-0.09	482.54	0.38	-0.66	524.55	0.31	-0.67	526.83	0.31
Median	-1.43	413.84	0.07	-0.77	361.42	0.08	-1.58	433.10	0.00	-1.59	434.64	-0.01
Minimum	-5.14	324.65	-0.21	-1.75	277.78	-0.24	-2.79	343.72	-0.29	-2.81	344.30	-0.29

271 In the same way as with the number of rainy days, the difference between the total precipitation per hydrological year estimated
 272 from observed data and downscaled data is associated with underestimations and overestimations. When no downscaling
 273 technique is applied, an underestimation of total precipitation per hydrological year is observed. However, when DM, QM, or
 274 RT is applied, this underestimation changes to overestimation (see Figure 5).

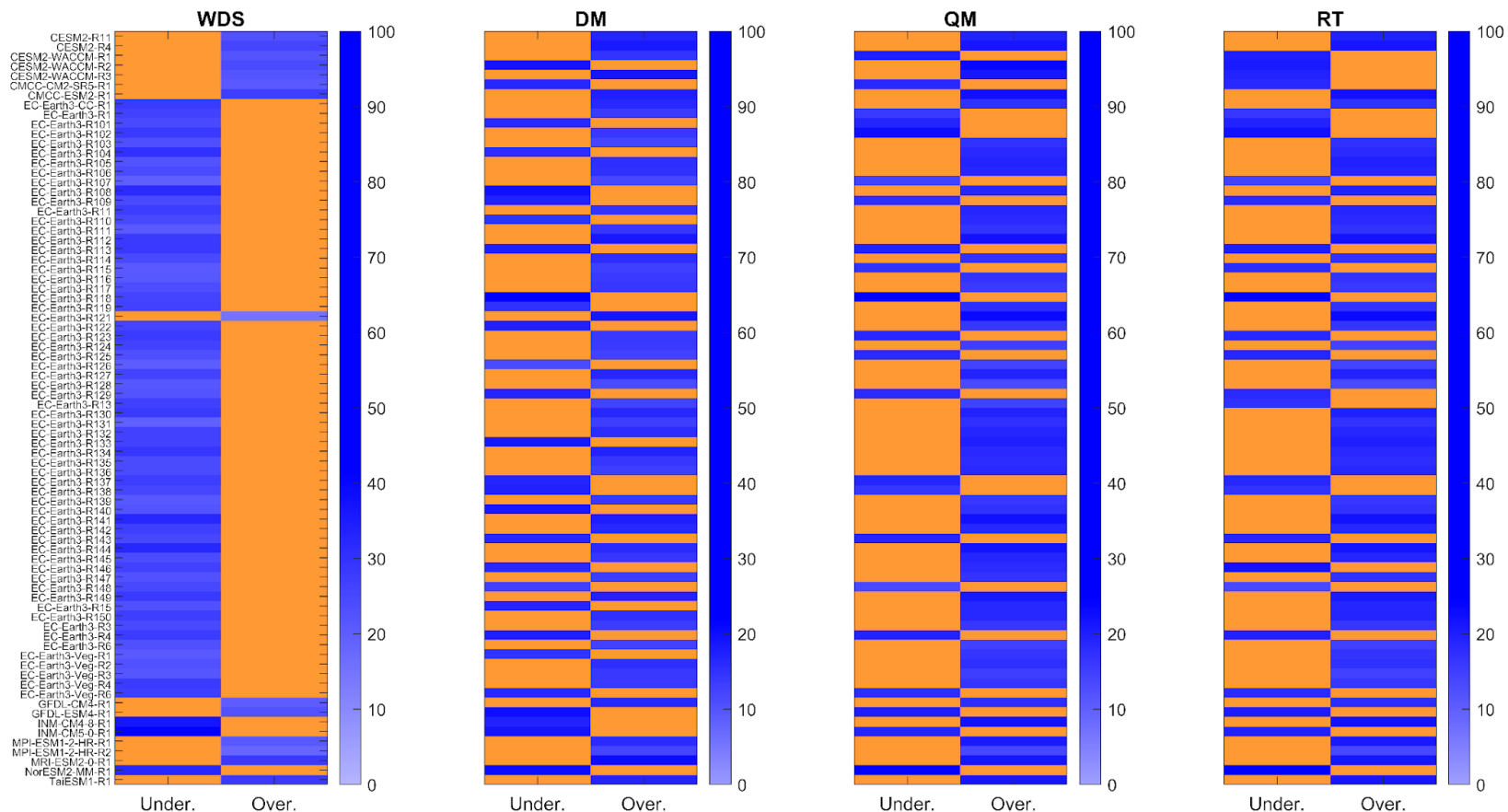
275 In the case of QM and RT, the overestimation of total hydrological precipitation per year (Figure 4) is related to the
 276 overestimation of the number of rainy days (Figure 3) most of the time. Thus, it is noticeable that the application of QM and
 277 RT increases both the number of rainy days in the hydrological year and the magnitudes of simulated precipitations. However,
 278 this trend is intrinsic to the conceptual foundation of these methods. For example, during the application of QM or RT, a
 279 simulated quantile of 1 mm of rain can be associated with an observed quantile of 20 mm of rain.

280 The median percentage underestimation errors were 25.58%, 17,02%, 18.74%, and 18.77% for WDS, DM, QM, and RT,
 281 respectively. Meanwhile, the average overestimations were 22.37%, 14.63%, 18.37%, and 18.30% for WDS, DM, QM, and
 282 RT, respectively.



284

285 Figure 4 Median performance metrics (RMSE and R) for estimated total precipitation from series simulated by GCMs, without
 286 downscaling (WDS), as well as adjusted series obtained using the DM, QM, and RT.



287 Figure 5 Median percentage error of underestimation or overestimation of total precipitation per hydrological year. The percentage error of the
 288 prevailing condition of underestimation (Under.) or overestimation (Over.) is represented in blue, while the non-prevailing condition is depicted in
 289 orange. For example, if underestimation is prevalent, overestimation is represented in orange. **WDS represents the condition without the application**
 290 **of downscaling techniques, DM corresponds to the condition when the Delta Method is applied, QM represents the condition when Quantile**
 291 **Mapping is applied, and RT indicates the condition of applying Regression Trees as a downscaling technique.**

292 **3.2 Total precipitation and number of rainy days at multiyear level.**

293 In the multiyear context, estimates derived from downscaled series using DM, QM, and RT showed more robust agreement
294 with the estimations made from the historical records compared to the annual scale. A low discrepancy between the number
295 of rainy days and total precipitation was observed at the multiyear scale.

296 When examining the number of rainy days, it was noted that the smallest errors are achieved when employing QM and RT as
297 downscaling techniques. Additionally, estimates derived from downscaled series through DM demonstrated a performance
298 similar to cases where no downscaling technique was applied (see Figure 6 and Table 4). Thus, in the multiyear scale, the
299 series adjusted by QM yielded the smallest percentage errors, followed by those adjusted by RT and DM.

300 Table 4 Summary of percentual errors of number of rainy days in the multiyear level.

	SDS	DM	QM	RT
Maximum	141.90%	116.78%	1.21%	2.58%
Median	83.90%	77.88%	0.60%	1.83%
minimum	21.56%	1.20%	0.27%	1.19%

301 On the other hand, it was observed that the estimation of total precipitation at the multiyear scale, from series downscaled by
302 DM, QM, and RT, significantly reduces percentage errors compared to cases where no downscaling technique is applied (See
303 Figure 7 and Table 5).

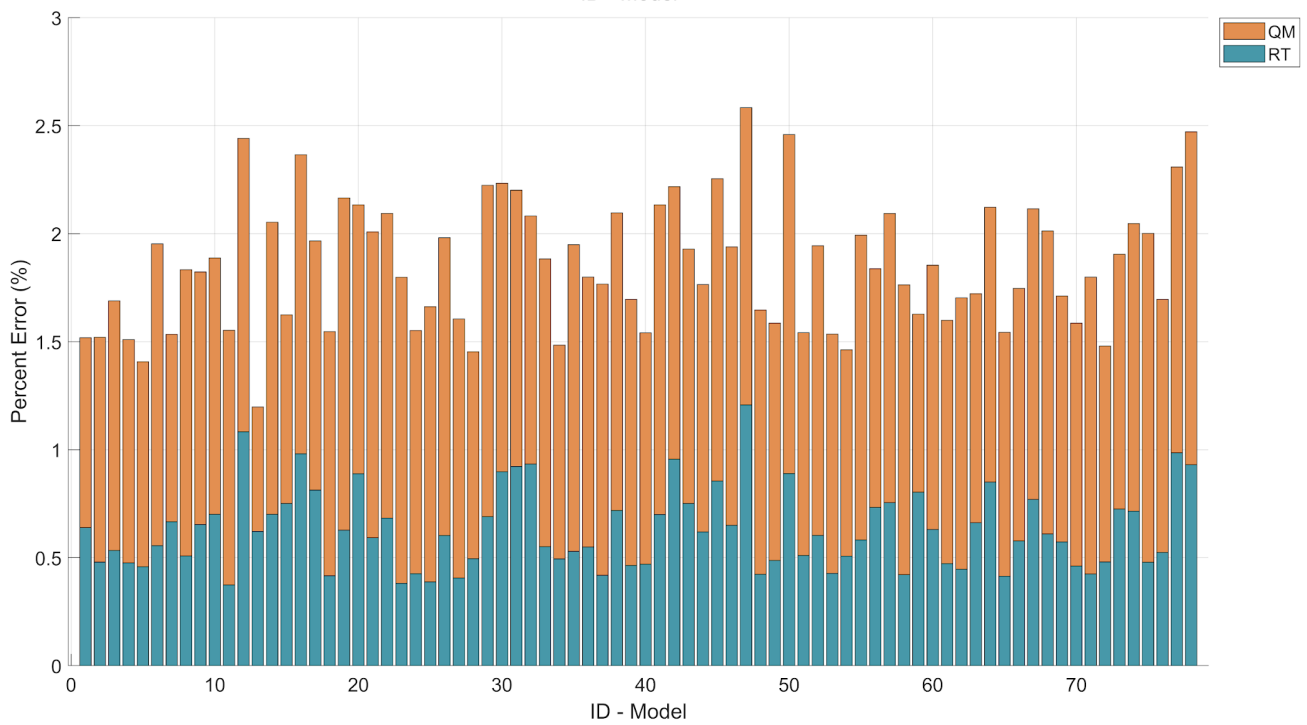
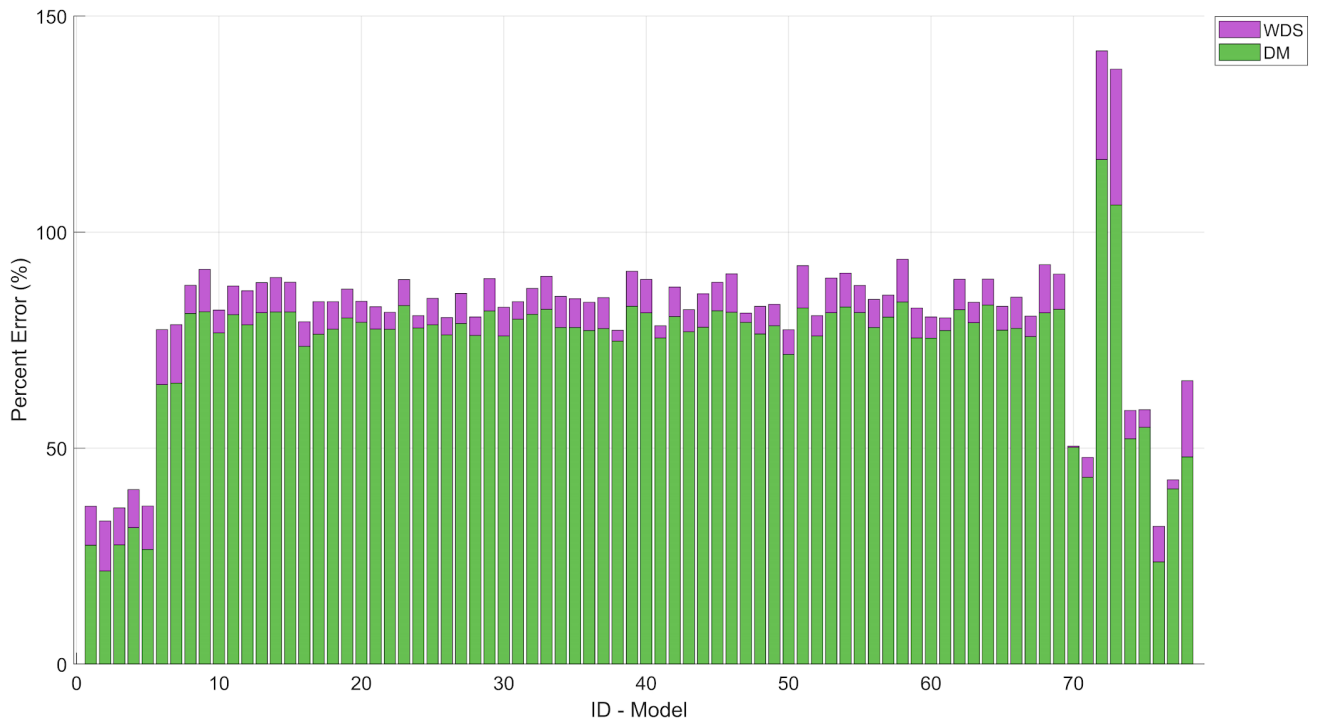
304 Table 5 Summary of percentual errors of total precipitation in the multiyear level.

	SDS	DM	QM	RT
Maximum	33.59%	1.55%	1.99%	1.83
Median	12.13%	0.81%	1.02%	0.89
minimum	7.62%	0.43%	0.00%	0.01

305
306 Based on the results, employing downscaled series for estimating total precipitation and the number of rainy days on a
307 hydrological year scale demonstrates better performance in the multi-year context. Therefore, it is recommended to utilize
308 downscaled series by employing DM, QM, and RT for estimating total precipitation and the number of rainy days at the multi-
309 year scale.

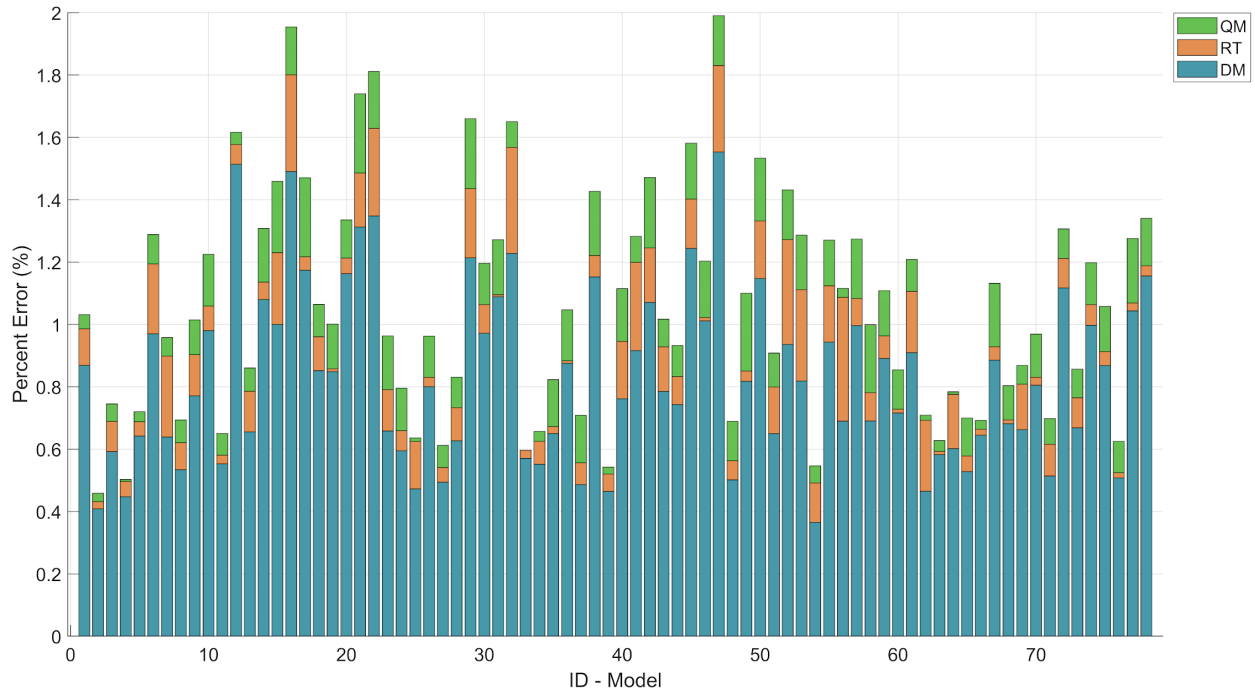
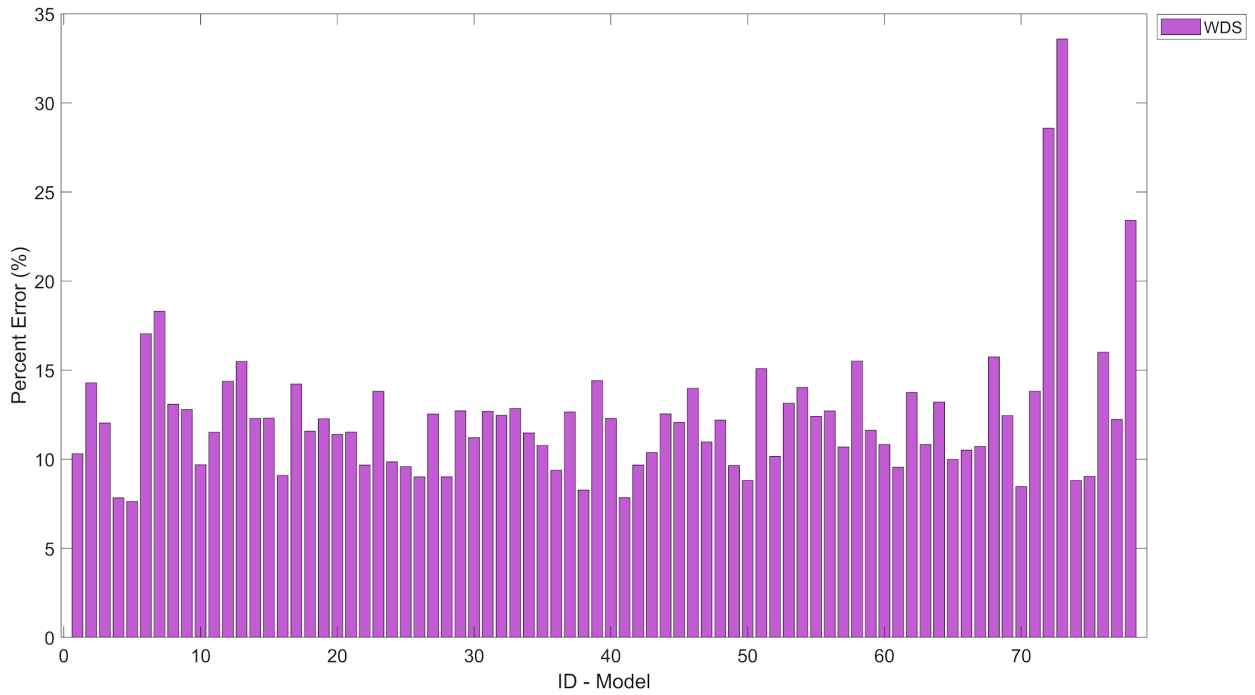
310
311 **It was observed that the performance of downscaling techniques at the annual scale was consistently reflected at the multiyear**
312 **scale.** Regarding the number of rainy days, the QM method demonstrated superior performance across both annual and
313 multiyear scales. As for total precipitation per hydrological year, the DM method showcased the best performance, exhibiting
314 even higher efficiency at the multiyear scale.

315



316
317
318
319

Figure 6 Median of Percentage Errors of Rainy Days at the multiyear level to each model. Without the application of downscaling techniques (WDS), and with the application of Delta Method (DM), Quantile Mapping (QM), and Regression Trees (RT) as downscaling techniques.



321

322 Figure 7 Median of Percentage Errors of total precipitation at the multiyear level to each model. Without the application of
 323 downscaling techniques - WDS, and with the application of Delta Method - DM, Quantile Mapping - QM, and Regression
 324 Trees - RT as downscaling techniques.

326 **3.1 Frequency Analysis**

327 Developed frequency analyses from downscaled series using QM and RT yield satisfactory results, evidenced by good
 328 performance in the NSE and KGE metrics. With respect to the frequency analyses developed from series downscaled by the
 329 DM method, it is observed that the results were comparable to those obtained when no downscaling technique was applied
 330 (see Figure 8 and Table 6).

331 Figure 8 illustrates a significant improvement in yield metrics following the implementation of QM and RT. The metrics
 332 approach unity, suggesting that the quantiles estimated from the adjusted series closely align with those derived from the
 333 historical series.

334 The percentage errors obtained in the estimates made with series downscaled by QM and RT were less than 12.18% and 5.91%,
 335 respectively. In contrast, the errors in the estimates made with series downscaled by the DM method were similar to those
 336 obtained when no downscaling technique was applied (See Table 6).

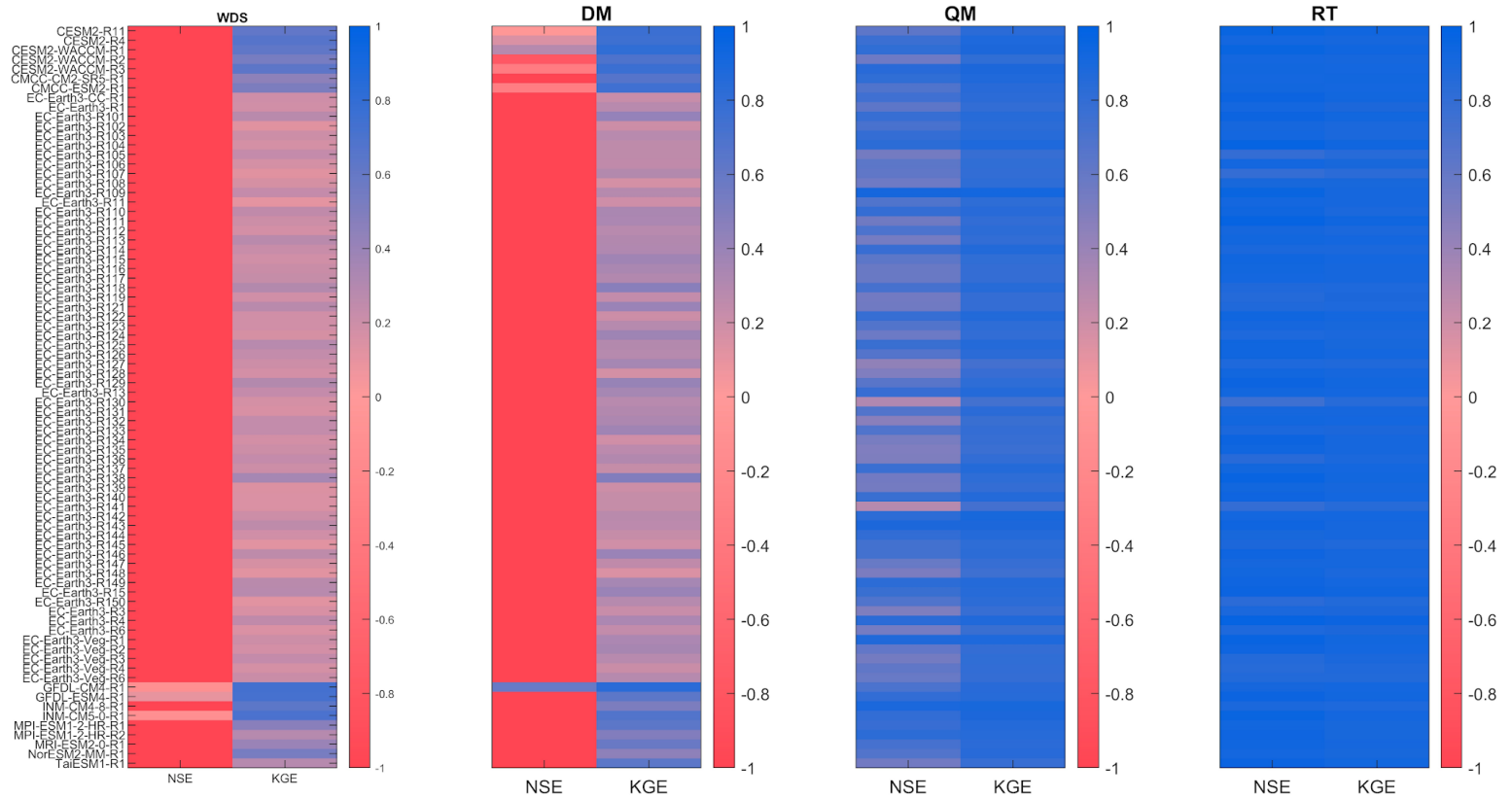
337 Table 6 Summary of percentual errors obtained in the Frequency analysis.

	SDS	DM	QM	RT
Maximum	57.95%	55.9%	12.18%	5.91%
Median	52.69%	47.1%	7.38%	1.56%
minimum	1.97%	0.45%	1.21%	0.09%

338 The high performance achieved in the estimation of quantiles from adjusted series through QM and RT is associated with the
 339 fact that the largest quantiles simulated by GCMs are correlated with the largest observed quantiles. Consequently, observed
 340 and simulated series of maximum values end up close values. This fact leads to comparable outcomes in estimations, regardless
 341 of whether they are derived from observed or downscaled series.

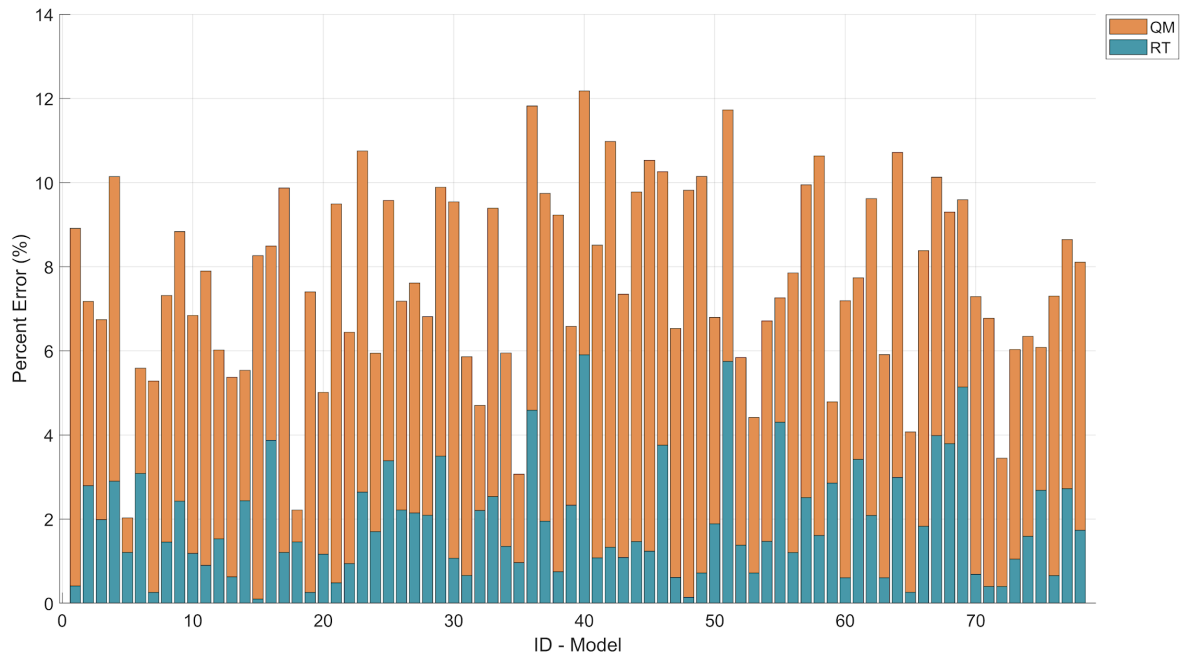
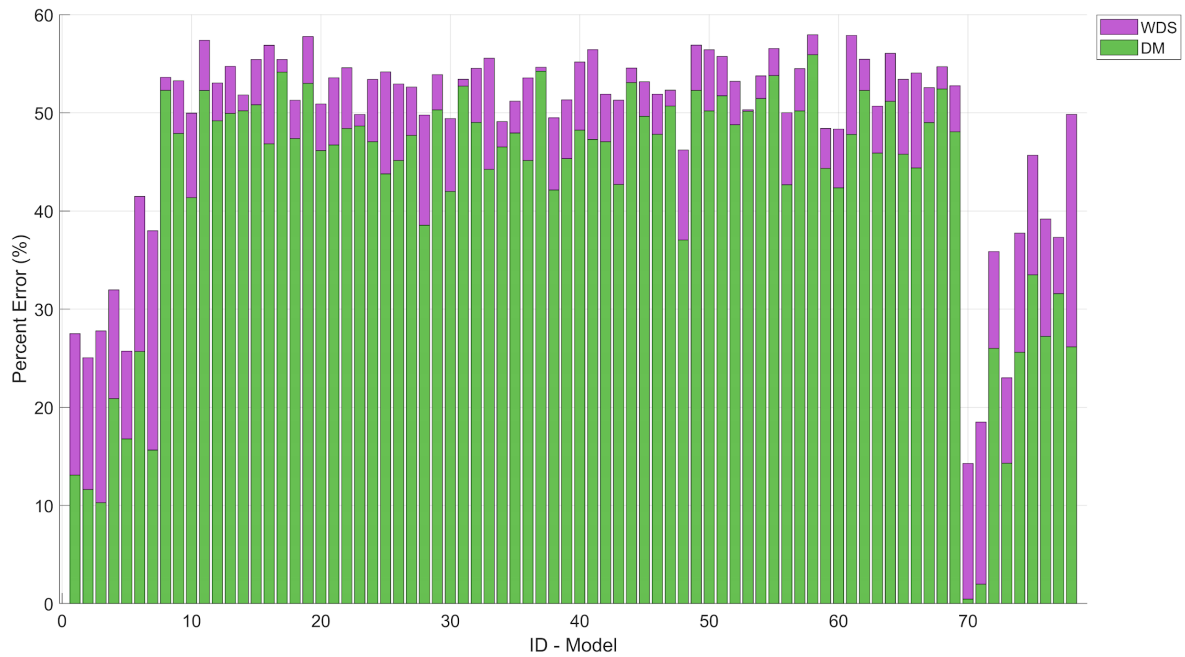
342 Given that downscaling in the case of DM is accomplished through the application of factors, the difference between the
 343 maximum precipitation observed and estimated from the adjusted series is substantial. Consequently, this results in a
 344 significant disparity in the outcomes of frequency analysis.

345 It was evident that the dispersion and variability of estimated quantiles from the adjusted series increased as the return period
 346 extended; however, this must be associated with the low occurrence of quantiles with high return times in the historical series
 347 (See Figure 10). Additionally, it was observed that errors related to DM are associated with an underestimation of quantiles
 348 for different return periods. Thus, it is concluded that the development of frequency analyses from adjusted series through QM
 349 and RT is feasible, with RT emerging as the technique that exhibited the best performance.



350

351 Figure 8 Median performance metrics (NSE e KGE) for the frequency analysis developed from precipitation series simulated by GCMs, without
 352 the application of downscaling techniques (WDS), as well as adjusted series obtained using the Delta Method (DM), Quantile Mapping (QM), and
 353 Regression Trees (RT).
 354



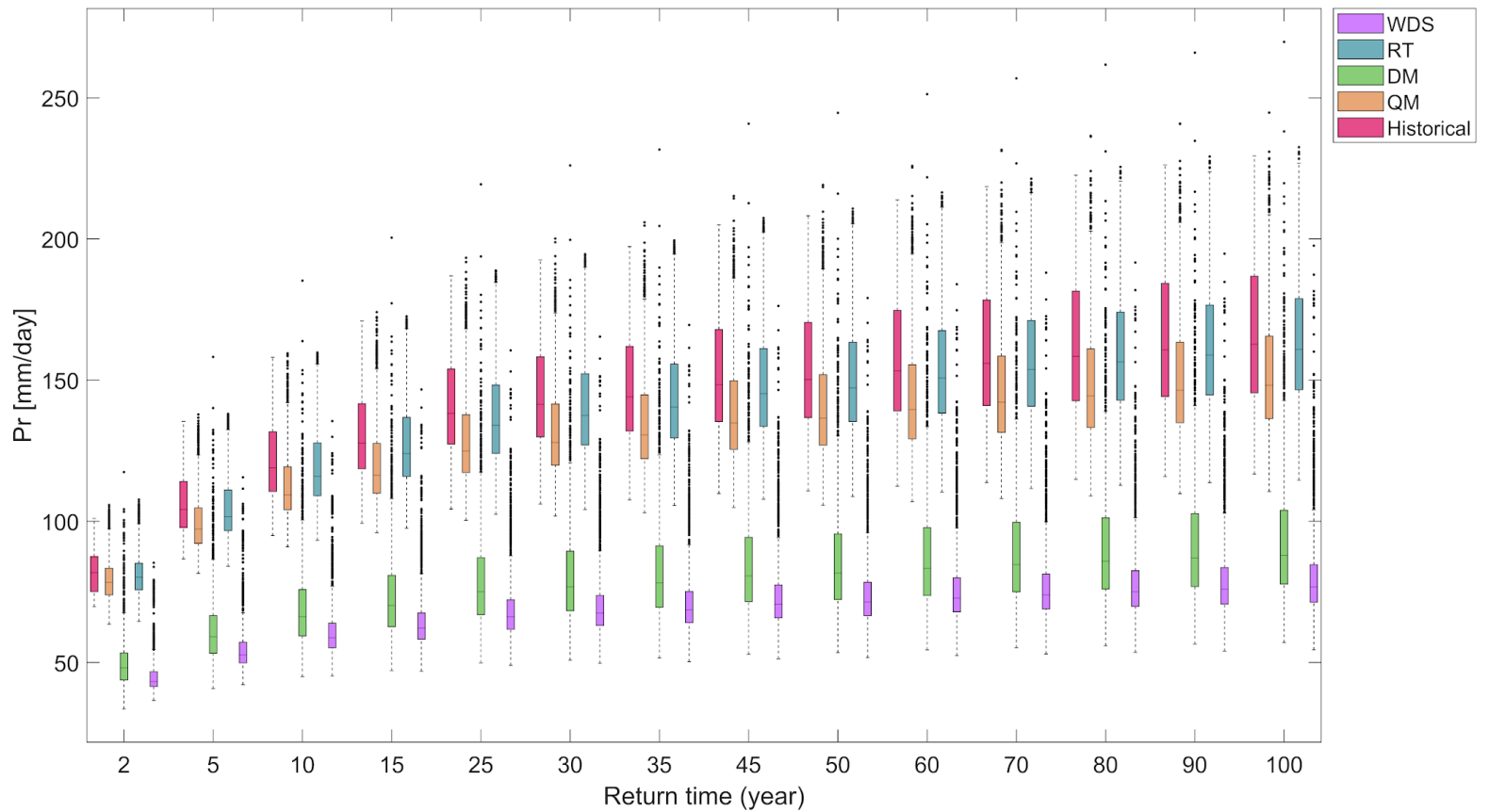
356

357

358

359

Figure 9 Median of percentual error obtained in the frequency analysis developed from precipitation series simulated by GCMs, without the application of downscaling techniques WDS, as well as reduced series obtained using the Delta Method - DM, Quantile Mapping - QM, and Regression Trees - RT.



360
361
362
363

Figure 10 Frequency analysis developed from precipitation series simulated by GCMs, without the application of downscaling techniques (WDS), as well as adjusted series obtained using the Delta Method (DM), Quantile Mapping (QM), and Regression Trees (RT) for the return time of 2, 5, 10, 15, 25, 30, 35, 45, 50, 60, 70, 80, 90 and 100 years.

364 4. Conclusions

365 This study aimed to assess the performance of using downscaled series through the Delta Method, Quantile Mapping, and
366 Regression Trees to develop frequency analysis and estimate total precipitation and the number of rainy days per hydrological
367 year at annual and multiyear levels.

368 It was observed that the Global Climate Models (GCMs) from the sixth phase of the Coupled Model Intercomparison Project
369 (CMIP6) underestimated the number of rainy days per hydrological year for MRBH, with a median of 78 days. When
370 estimating the number of rainy days from the downscaled series by DM, the tendency of underestimation persists and
371 insignificantly decreases to 73 days. It was also observed that, when employing downscaled series through the application of
372 QM and RT, underestimation is reversed to a slight overestimation. The average overestimations were 18 days for QM and
373 19 days for RT. Despite the relatively low magnitude of overestimations, the low NSE and KGE scores suggest that estimating
374 the number of rainy days at an annual scale from downscaled series using DM, QM, and RT does not guarantee accurate
375 results.

376 Similarly, GCMs underestimate total precipitation for the hydrological year, with a median of 413.84 mm. The use of a
377 downscaled series by the DM reduces this difference to 361.42 mm. However, when QM and RT are applied, the differences
378 surpass those without downscaling. The median differences in those cases are 433.10 mm for QM and 434.64 mm for RT.
379 These facts, along with the low NSE and KGE scores, suggest that annual estimations of the number of rainy days and total
380 precipitation from downscaled series by DM, QM, and RT do not yield reliable results. This result is also due to the fact that
381 a one-year time window is not optimal for analysing the precipitation simulated by the considered RCMs, and consequently,
382 more significant results were found with the multiyear study.

383 Therefore, at the multiyear scale, the estimation of the number of rainy days and total precipitation demonstrated high
384 performance. For the number of rainy days, the percentage errors between the magnitudes of the total estimated from adjusted
385 and observed series were less than 1.21% and 2.58% when downscaled series by QM and RT were employed. Percentage
386 errors for estimating total rainfall per hydrological year on a multiyear scale were 1.55%, 1.99%, and 1.83% when downscaled
387 series by DM, QM, and RT were used, respectively.

388 Finally, developing frequency analysis from the daily precipitation simulated by the MCGs allows obtaining quantiles close
389 to those estimated with historical records when QM and RT are applied. The performance achieved in estimating quantiles
390 from adjusted series by QM and RT is attributed to the fact that QM and RT associate the largest quantiles simulated by GCMs
391 with the largest observed quantiles. As a result, observed and downscaled series have close values. The percentage error of
392 estimates made from downscaled series by QM and RT, in relation to estimates based on observed data, were lower than

393 12.18% and 5.91%, respectively. In this context, it is recommended to utilize downscaling based on RT when the goal is to
394 assess future changes in frequency of occurrence.

395 **References**

396

397 Fadhel, S., Rico-Ramirez, M. A., & Han, D. (2017). Uncertainty of Intensity–Duration–Frequency (IDF) curves due to varied
398 climate baseline periods. *Journal of Hydrology*, 547, 600–612. <https://doi.org/10.1016/j.jhydrol.2017.02.013>

399 Ghasemi Tousi, E., O’Brien, W., Doulabian, S., & Shadmehri Toosi, A. (2021). Climate changes impact on stormwater
400 infrastructure design in Tucson Arizona. *Sustainable Cities and Society*, 72, 103014.
401 <https://doi.org/10.1016/j.scs.2021.103014>

402 Gupta, H. V., Kling, H., Yilmaz, K. K., & Martinez, G. F. (2009). Decomposition of the mean squared error and NSE
403 performance criteria: Implications for improving hydrological modelling. *Journal of Hydrology*, 377(1–2), 80–91.
404 <https://doi.org/10.1016/j.jhydrol.2009.08.003>

405 Hashmi, M. Z., Shamseldin, A. Y., & Melville, B. W. (2011). Statistical downscaling of watershed precipitation using Gene
406 Expression Programming (GEP). *Environmental Modelling & Software*, 26(12), 1639–1646.
407 <https://doi.org/10.1016/j.envsoft.2011.07.007>

408 Hassanzadeh, E., Nazemi, A., & Elshorbagy, A. (2014). Quantile-Based Downscaling of Precipitation Using Genetic
409 Programming: Application to IDF Curves in Saskatoon. *Journal of Hydrologic Engineering*, 19(5), 943–955.
410 [https://doi.org/10.1061/\(ASCE\)HE.1943-5584.0000854](https://doi.org/10.1061/(ASCE)HE.1943-5584.0000854)

411 Heo, J.-H., Ahn, H., Shin, J.-Y., Kjeldsen, T. R., & Jeong, C. (2019). Probability Distributions for a Quantile Mapping
412 Technique for a Bias Correction of Precipitation Data: A Case Study to Precipitation Data Under Climate Change.
413 *Water*, 11(7), 1475. <https://doi.org/10.3390/w11071475>

414 Hutengs, C., & Vohland, M. (2016). Downscaling land surface temperatures at regional scales with random forest regression.
415 *Remote Sensing of Environment*, 178, 127–141. <https://doi.org/10.1016/j.rse.2016.03.006>

- 416 IPCC, I. P. on C. C. (2014). *Climate Change 2014 Mitigation of Climate Change: Working Group III Contribution to the Fifth*
417 *Assessment Report of the Intergovernmental Panel on Climate Change.*
418 https://www.ipcc.ch/site/assets/uploads/2018/02/ipcc_wg3_ar5_frontmatter.pdf
- 419 Jakob Themeßl, M., Gobiet, A., & Leuprecht, A. (2011). Empirical-statistical downscaling and error correction of daily
420 precipitation from regional climate models. *International Journal of Climatology*, 31(10), 1530–1544.
421 <https://doi.org/10.1002/joc.2168>
- 422 Jimenez, D. A. (2022). *Avaliação das alterações nas frequências de ocorrência das precipitações diárias máximas para a*
423 *região Metropolitana de Belo Horizonte considerando diferentes cenários de climas futuros.* [Universidade Federal
424 de Minas Gerais - UFMG]. <https://repositorio.ufmg.br/handle/1843/46268>
- 425 Khalid, I. A., & Sitanggang, I. S. (2022). *Machine Learning-Based Spatial Downscaling on Precipitation Satellite Data in*
426 *Riau Province, Indonesia.* 10.
- 427 Kreienkamp, F., Paxian, A., Früh, B., Lorenz, P., & Matulla, C. (2019). Evaluation of the empirical–statistical downscaling
428 method EPISODES. *Climate Dynamics*, 52(1), 991–1026. <https://doi.org/10.1007/s00382-018-4276-2>
- 429 Liu, W., Bailey, R. T., Andersen, H. E., Jeppesen, E., Nielsen, A., Peng, K., Molina-Navarro, E., Park, S., Thodsen, H., &
430 Trolle, D. (2020). Quantifying the effects of climate change on hydrological regime and stream biota in a
431 groundwater-dominated catchment: A modelling approach combining SWAT-MODFLOW with flow-biota empirical
432 models. *Science of The Total Environment*, 745, 140933. <https://doi.org/10.1016/j.scitotenv.2020.140933>
- 433 Loh, W. (2011). Classification and regression trees. *WIREs Data Mining and Knowledge Discovery*, 1(1), 14–23.
434 <https://doi.org/10.1002/widm.8>
- 435 Mahla, P., Lohani, A. K., Chandola, V. K., Thakur, A., Mishra, C. D., & Singh, A. (2019). Downscaling Of Precipitation Using
436 Statistical Downscaling Model and Multiple Linear Regression Over Rajasthan State. *Current World Environment*,
437 14(1), 68–98. <https://doi.org/10.12944/CWE.14.1.09>
- 438 Mann, H. B., & Whitney, D. R. (1947). On the test of whether one of random variables is stochastically larger than the other.
439 *Annals of Mathematical Statistics.*
- 440 Naghettini, M., & Pinto, É. J. (2007). *Hidrologia Estatística.* CPRM.

441 Nash, J. E., & Sutcliffe, J. V. (1979). *River flow forecasting through conceptual models part I — A discussion of principles—*
442 *ScienceDirect*. [https://doi.org/10.1016/0022-1694\(70\)90255-6](https://doi.org/10.1016/0022-1694(70)90255-6)

443 NERC, N. E. R. C. (1975). *Flood Studies Report*.

444 Norris, J., Chen, G., & Li, C. (2020). Dynamic Amplification of Subtropical Extreme Precipitation in a Warming Climate.
445 *Geophysical Research Letters*, 47(14). <https://doi.org/10.1029/2020GL087200>

446 Olsson, J., Arheimer, B., Borris, M., Donnelly, C., Foster, K., Nikulin, G., Persson, M., Perttu, A.-M., Uvo, C., Viklander, M.,
447 & Yang, W. (2016). Hydrological Climate Change Impact Assessment at Small and Large Scales: Key Messages
448 from Recent Progress in Sweden. *Climate*, 4(3), 39. <https://doi.org/10.3390/cli4030039>

449 Onyutha, C., Tabari, H., Rutkowska, A., Nyeko-Ogiramoi, P., & Willems, P. (2016). Comparison of different statistical
450 downscaling methods for climate change rainfall projections over the Lake Victoria basin considering CMIP3 and
451 CMIP5. *Journal of Hydro-environment Research*, 12, 31–45. <https://doi.org/10.1016/j.jher.2016.03.001>

452 Ostad-Ali-Askari, K., Ghorbanizadeh Kharazi, H., Shayannejad, M., & Zareian, M. J. (2020). Effect of Climate Change on
453 Precipitation Patterns in an Arid Region Using GCM Models: Case Study of Isfahan-Borkhar Plain. *Natural Hazards*
454 *Review*, 21(2), 04020006. [https://doi.org/10.1061/\(ASCE\)NH.1527-6996.0000367](https://doi.org/10.1061/(ASCE)NH.1527-6996.0000367)

455 Ozbuldu, M., & Irvem, A. (2021). Evaluating the effect of the statistical downscaling method on monthly precipitation
456 estimates of global climate models. *Global NEST Journal*, 23(2), 232–240. <https://doi.org/10.30955/gnj.003458>

457 Rastogi, D., Kao, S.-C., & Ashfaq, M. (2022). How May the Choice of Downscaling Techniques and Meteorological Reference
458 Observations Affect Future Hydroclimate Projections? *Earth's Future*, 10(8), e2022EF002734.
459 <https://doi.org/10.1029/2022EF002734>

460 Riahi, K., van Vuuren, D. P., Kriegler, E., Edmonds, J., O'Neill, B. C., Fujimori, S., Bauer, N., Calvin, K., Dellink, R., Fricko,
461 O., Lutz, W., Popp, A., Cuaresma, J. C., Kc, S., Leimbach, M., Jiang, L., Kram, T., Rao, S., Emmerling, J., ... Tavoni,
462 M. (2016). The Shared Socioeconomic Pathways and their energy, land use, and greenhouse gas emissions
463 implications: An overview. *Global Environmental Change*, 42, 153–168.
464 <https://doi.org/10.1016/j.gloenvcha.2016.05.009>

- 465 Roca, V., B., Beltrán, S. M., & Gómez, H. R. (2019). Cambio climático y salud. *Revista Clínica Española*, 219(5), 260–265.
466 <https://doi.org/10.1016/j.rce.2019.01.004>
- 467 Sachindra, D. A., Ahmed, K., Rashid, Md. M., Shahid, S., & Perera, B. J. C. (2018). Statistical downscaling of precipitation
468 using machine learning techniques. *Atmospheric Research*, 212, 240–258.
469 <https://doi.org/10.1016/j.atmosres.2018.05.022>
- 470 Sachindra, D. A., Ahmed, K., Shahid, S., & Perera, B. J. C. (2018). Cautionary note on the use of genetic programming in
471 statistical downscaling. *International Journal of Climatology*, 38(8), 3449–3465. <https://doi.org/10.1002/joc.5508>
- 472 Salehnia, N., Hosseini, F., Farid, A., Kolsoumi, S., Zarrin, A., & Hasheminia, M. (2019). Comparing the Performance of
473 Dynamical and Statistical Downscaling on Historical Run Precipitation Data over a Semi-Arid Region. *Asia-Pacific
474 Journal of Atmospheric Sciences*, 55(4), 737–749. <https://doi.org/10.1007/s13143-019-00112-1>
- 475 Salehnia, N., Salehnia, N., Saradari Torshizi, A., & Kolsoumi, S. (2020). Rainfed wheat (*Triticum aestivum* L.) yield prediction
476 using economical, meteorological, and drought indicators through pooled panel data and statistical downscaling.
477 *Ecological Indicators*, 111, 105991. <https://doi.org/10.1016/j.ecolind.2019.105991>
- 478 Shahabul Alam, Md., & Elshorbagy, A. (2015). Quantification of the climate change-induced variations in Intensity–Duration–
479 Frequency curves in the Canadian Prairies. *Journal of Hydrology*, 527, 990–1005.
480 <https://doi.org/10.1016/j.jhydrol.2015.05.059>
- 481 Tabari, H., Paz, S. M., Buekenhout, D., & Willems, P. (2021). Comparison of statistical downscaling methods for climate
482 change impact analysis on precipitation-driven drought. *Hydrology and Earth System Sciences*, 25(6), 3493–3517.
483 <https://doi.org/10.5194/hess-25-3493-2021>
- 484 Teutschbein, C., & Seibert, J. (2012). Bias correction of regional climate model simulations for hydrological climate-change
485 impact studies: Review and evaluation of different methods. *Journal of Hydrology*, 456–457, 12–29.
486 <https://doi.org/10.1016/j.jhydrol.2012.05.052>
- 487 Teutschbein, C., Wetterhall, F., & Seibert, J. (2011). Evaluation of different downscaling techniques for hydrological climate-
488 change impact studies at the catchment scale. *Climate Dynamics*, 37(9–10), 2087–2105.
489 <https://doi.org/10.1007/s00382-010-0979-8>

- 490 Waters, D., Watt, W. E., Marsalek, J., & Anderson, B. C. (2003). Adaptation of a Storm Drainage System to Accommodate
491 Increased Rainfall Resulting from Climate Change. *Journal of Environmental Planning and Management*, 46(5),
492 755–770. <https://doi.org/10.1080/0964056032000138472>
- 493 Worku, G., Teferi, E., Bantider, A., & Dile, Y. T. (2021). Modelling hydrological processes under climate change scenarios
494 in the Jemma sub-basin of upper Blue Nile Basin, Ethiopia. *Climate Risk Management*, 31, 100272.
495 <https://doi.org/10.1016/j.crm.2021.100272>
- 496 Yang, Y., Tang, J., Xiong, Z., Wang, S., & Yuan, J. (2019). An intercomparison of multiple statistical downscaling methods
497 for daily precipitation and temperature over China: Present climate evaluations. *Climate Dynamics*, 53(7), 4629–
498 4649. <https://doi.org/10.1007/s00382-019-04809-x>
- 499 Zhang, Z., & Li, J. (2020). Big climate data. Em *Big Data Mining for Climate Change* (p. 1–18). Elsevier.
500 <https://doi.org/10.1016/B978-0-12-818703-6.00006-4>